Contribution from the Transuranium Research Laboratory, Oak Ridge National Laboratory, Oak Ridge, Tennessee 37830, and Departments of Chemistry and Physics, Baylor University, Waco, Texas 76703

Reinterpretation of the Structural and Physical Property Changes in the Dehydration of Co$_3$[Co(CN)$_6$]$_2$·12H$_2$O

G. W. BEALL,* D. F. MULLICA, and W. O. MILLIGAN

A new structural model for M$_3$[Co(CN)$_6$]$_2$·nH$_2$O, where M = Co and other divalent metals and n = 12–14, has allowed an improved interpretation for the color change resulting from the dehydration of Co$_3$[Co(CN)$_6$]$_2$·12H$_2$O to be formed. The model permits an explanation of frequency shifts in visible spectra and other available and related studies which is all inclusive with experimental data.

Introduction

A tremendous amount of work has been accomplished in the past on Prussian blue and its analogues. The majority of these studies have been conducted on precipitated powder samples owing to the low solubility of these compounds. The structural model employed in these studies was proposed by Weiser, Milligan, and Bates,[1] which was derived from powder diffraction patterns. A study by Shriver and Brown[2] employed this model to interpret a peculiar reversible color change that occurs in Co$_3$[Co(CN)$_6$]$_2$·12H$_2$O upon dehydration. New structural data obtained on Mn$_3$[Co(CN)$_6$]$_2$·12H$_2$O and Cd$_3$[Co(CN)$_6$]$_2$·12H$_2$O employing both single-crystal X-ray and neutron diffraction by Beall et al.[3] indicate that the proposed interpretation of Shriver et al.[2] is no longer adequate. This new structural information has prompted this paper and an improved mechanism for the phenomena.

Experimental Section

Crystals employed in our studies were grown by the slow diffusion U-tube method from dilute solutions of CoCl$_2$ and freshly prepared H$_3$Co(CN)$_6$. The powder compounds used for lattice-constant determinations were precipitated by mixing stoichiometric amounts of CoCl$_2$ and H$_3$Co(CN)$_6$ solutions. These precipitated powders were washed many times with use of centrifugation to remove excess ion contamination. The lattice constants were determined by using a Siemens Debye–Scherrer cylindrical powder camera (114.8 mm, nickel-filtered Cu Kα radiation, mean λ = 1.5418 Å) and a least-square program[4] that utilizes the Nelson–Riley extrapolation function. Thermal dehydration results of 12–14 water molecules per formula unit were obtained on a Perkin-Elmer TGS-1 thermobalance. A Cary 82 spectrometer and a Spectra Physics Model 164 krypton-ion laser (6421-Å line) were used to obtain Raman data, mentioned here within, and a Perkin-Elmer 521 grating infrared spectrometer over the frequency range of 4000–250 cm^{-1} was employed to confirm dehydration as well as to identify the broad hydrogen-bonding band.

Results and Discussion

As mentioned, earlier work by Shriver and Brown[2] led to some conclusions as to the mechanisms of the color transition that occurs when Co$_3$[Co(CN)$_6$]$_2$·12H$_2$O is dehydrated. These conclusions in light of new structural data[3] indicate the conclusions were drawn on an incorrect structural model. A detailed comparison of the two structural models seems appropriate. The structural model employed by Shriver and Brown[2] was derived from powder diffraction data. It consists of a cubic framework composed of Co(CN)$_6^{3-}$ octahedra linked by Co^{2+} atoms. In addition to these two types of Co atoms, there was a third type of Co atom contained in the center of cubes formed by the Co—C≡N—Co linkages. This interstitial Co atom was believed to be octahedrally coordinated by water molecules. This model would result in four Co^{3+}–(C)$_6$, four Co^{2+}–(N)$_6$, and two Co^{2+}–(H$_2$O)$_6$, all octa-

Table I. Lattice Constants of M$_3$[Co(CN)$_6$]$_2$·nH$_2$O^a

M(II)	$a_0,^b$ Å	$a_0,^c$ Å	$a_0,^d$ Å
Cd (hydr)	10.600 (3)		10.590 (5)
Cd (dehydr)	10.46 (1)		
Mn (hydr)	10.436 (3)		10.43 (1)
Mn (dehydr)	10.22 (1)		
Fe (hydr)	10.308 (2)		10.31 (1)
Zn (hydr)	10.268 (3)		10.26 (1)
Co (pink, hydr)	10.228 (9)	10.17	10.210 (5)
Co (blue, dehydr)	10.161 (12)	10.16	

^{a} M(II) = Cd, Mn, Fe, Zn, and Co, and n has been experimentally shown to be 12 for Cd, Mn, Fe, and Zn (12–14 for Co) complexes. ^{b} This work and ref 3, 5, 6, and 8. ^{c} Reference 2. ^{d} Reference 11.

hedrally coordinated, per unit cell yielding a resultant formula of Co$_3$[Co(CN)$_6$]$_2$·6H$_2$O.

The structural model employed in this work is described in detail by Beall et al.[3] and has been given credence and verified in several crystallographic studies.[5-7] The cubic framework of this model is basically similar to that characterized by Shriver and Brown.[2] The differences arise mainly in the first Co^{3+} atom site. This 4a site ($Fm3m$, No. 225) is only occupied two-thirds of the time. This means that the Co^{2+} atoms linking the Co(CN)$_6$ groups would, on the average, have four nitrogens around them. The remaining coordinated sites on the Co^{2+} atoms are occupied by H$_2$O. There are no interstitial Co^{2+} atoms in the center of the cubes. This space is filled by water molecules of a zeolitic type which are believed to be hydrogen bonded into position as evidenced by IR studies. This structural model results in two types of Co atom coordination. The first being 2$^2/_3$ atoms/unit cell of Co^{3+}–(C)$_6$ that are octahedral and the second being 4 Co^{2+} atoms/unit cell of Co^{2+}–(N)$_4$(H$_2$O)$_2$ which is a slightly distorted octahedron owing to the difference between the bonding of the isocyanide and water. This structure results in a formula of Co$_3$[Co(CN)$_6$]$_2$·6H$_2$O which is identical with that proposed by the powder data. But, when the zeolitic waters are added to the formula that has been confirmed by both chemical analysis and dehydration isotherms, the result is Co$_3$[Co(CN)$_6$]$_2$·12–14H$_2$O. These two structures are illustrated in Figure 1.

Shriver and Brown[2] measured the lattice constants of both the hydrated pink form (10.17 Å) and the blue dehydrated

(1) H. B. Weiser, W. O. Milligan, and J. B. Bates, *J. Phys. Chem.,* **46,** 99 (1942).
(2) D. F. Shriver and D. B. Brown, *Inorg. Chem.,* **8,** 42 (1969).
(3) G. W. Beall, W. O. Milligan, J. Korp, and I. Bernal, *Inorg. Chem.,* **16,** 2715 (1977).
(4) R. B. Roof, Lattice Constant Refinement Program, LASL Report, Los Alamos Scientific Laboratory, Los Alamos, NM, 1968.
(5) D. F. Mullica, W. O. Milligan, G. W. Beall, and W. L. Reeves, *Acta Crystallogr., Sect. B,* **B34,** 3558 (1978).
(6) D. F. Mullica, J. D. Oliver, W. O. Milligan, and F. W. Hills, *Inorg. Nucl. Chem. Lett.,* in press.
(7) Unpublished results for Fe$_3$[Cr(CN)$_6$]$_2$·12H$_2$O and Cd$_3$[Cr(CN)$_6$]$_2$·14H$_2$O. The latter has been submitted.

*To whom correspondence should be addressed at the Transuranium Research Laboratory, Oak Ridge National Laboratory.
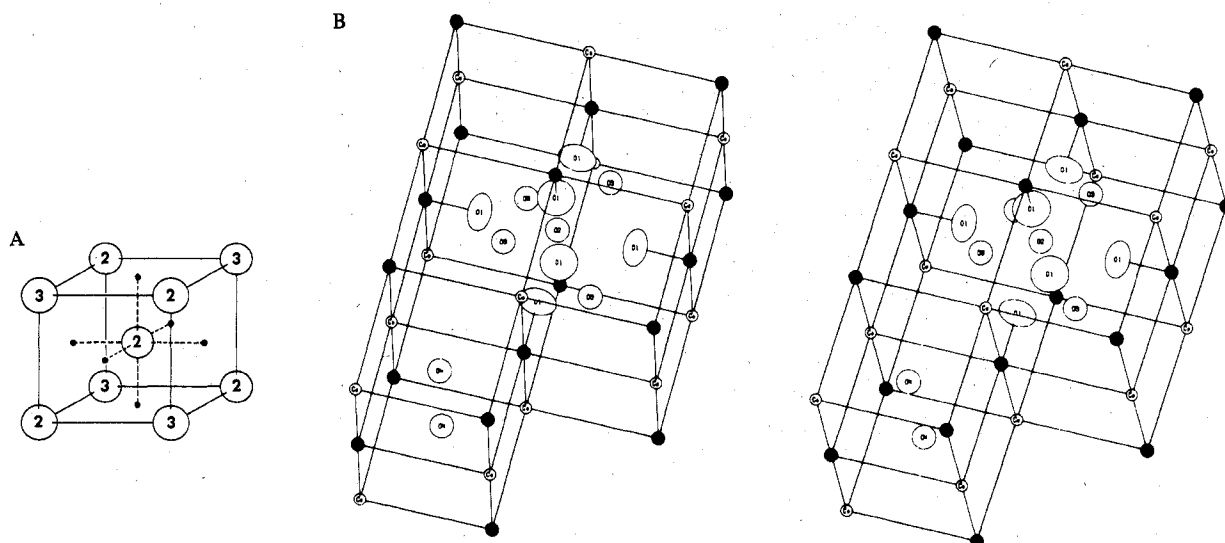
Figure 1. (A) Interstitial site in $Co_3[Co(CN)_6]_2$: (3) Co(III); (2) Co(II). The CN groups lie along the solid lines with the carbon ends toward Co(III). The central Co(II) atom is in an interstitial position.[2] (B) Stereoscopic view of the ordered and disordered structural representation of $M_3[Co(CN)_6]_2 \cdot 12H_2O$ (see ref 3 for detailed discussion). Filled circles (●) represent divalent transition metal, here Co(III). O(1) is bonded to Co(II), and O(2) is at the center of the cell surrounded by four O(3). O(4) is shown in the lower part of the figure.

form (10.16 Å). This small change in lattice constant upon dehydration is not completely in accord with our results. Both results are in discord with the experimental dehydration observations for $Mn_3[Co(CN)_6]_2 \cdot 12H_2O$ and $Cd_3[Co(CN)_6]_2 \cdot 12H_2O$[8] (see Table I). Shriver and Brown[2] observed a change in the vibration frequency of the cyanide upon dehydration (2177, 2139 cm^{-1} pink; 2183 cm^{-1} blue). This is in agreement with the shifts observed by Beall et al.[8] in a Raman vibration study of $Mn_3[Co(CN)_6]_2 \cdot 12H_2O$ where the hydrated form cyanide frequencies were $\gamma_1(A_{1g}) = 2190.3$ cm^{-1} and $\gamma_3(Eq) = 2171.4$ cm^{-1} and the frequencies associated with the dehydrated form were $\gamma_1 = 2201.4$ cm^{-1} and $\gamma_3 = 2178.0$ cm^{-1}.

Shriver and Brown[2] reported that the hydrated form has a maximum absorption at 470 nm and a sharp absorption band at 585 nm for the blue dehydrated form. This shift in the absorption spectra upon hydration was interpreted on the basis of the presence of interstitial $Co^{2+}-(H_2O)_6$ moieties. On the basis of the preceding discussion of the new structural model, this interpretation is unsatisfactory. The shift in the visible spectra can be explained more effectively by the change in the coordination polyhedron around the Co^{2+} atoms; i.e., after dehydration the polyhedron will change from nearly octahedral $Co^{2+}-(N)_4(H_2O)$ to $Co^{2+}-(N)_4$ which is a highly distorted tetrahedral coordination. This dehydration will be accompanied by an increase in the bond strength between the Co and N atoms and thus a noticeable observed decrease in the lattice constant (greater than 3 times the summation of the standard deviations (see Table I)) and a shift to higher frequencies in the vibrational spectra.

Some magnetic susceptibility data was also presented by Shriver and Brown.[2] A magnetic moment of 4.95 μ_B for Co^{2+} in the pink form was derived. This is in good agreement with what would be expected for a nearly octahedral $Co^{2+}-(N)_4(H_2O)_2$ moiety. When they attempted to interpret the magnetic data for the blue dehydrated form, an assumption was made that two-thirds of the Co^{2+} atoms would have a magnetic moment of 4.95 μ_B. This resulted in an unusually low moment for the remaining Co^{2+} atoms, 3.9 μ_B. This discrepancy disappears when the new structural model is employed. In this model, all the Co^{2+} atoms will have the same magnetic moment. This interpretation results in a magnetic moment of

4.6 μ_B for the Co^{2+} atom in the dehydrated form which is in excellent agreement with values of 4.5–4.7 μ_B for tetrahedral coordinated Co^{2+} atoms which are typically observed.[9,10]

Shriver and Brown[2] discussed the smooth dehydration isotherms observed by them and many others workers and made an attempt to explain why definite hydration breaks in the isotherms were not observed. A simple explanation can be seen when the detailed hydrogen-bonding network is examined in the structural model proposed by Beall et al.[3] It appears that the hydrogen-bonding network is important in stabilizing both the zeolitic and the coordinated water molecules. Thus, when some of the zeolitic water molecules begin to leave the lattice, the coordinated water molecules are also destablized and dehydrate in a smooth manner. This type of isotherm was observed in our thermal dehydration study (TGA) of the title compound.

An ammonia form of the $Co_3[Co(CN)_6]_2$ was also reported.[2] It was found that a definite break occurs at a composition of six NH_3's in the desorption isotherm. This is consistent with the fact that the NH_3 molecules would not form as strong a hydrogen-bonding network as the water molecules, and thus the zeolitic NH_3 molecules would not be held as tightly.

The cyanide vibrational frequencies for the hexaamine form are 2166 and 2125 cm^{-1} vs. 2177 and 2139 cm^{-1} in the hydrated form of cobalt(II) hexacyanocobaltate(III). This is in good agreement with the frequencies observed for the hydrated and amine forms of $Mn_3[Co(CN)_6]_2 \cdot X$ of 2190.3 and 2171.4 cm^{-1} and 2187.6 and 2170.9 cm^{-1}, respectively.[8]

In summary, after consideration of all available data and updated observed data which includes the newer and more accurate structural model derived from neutron and X-ray diffraction analyses,[3] an improved interpretation and explanation for the reversible color change occurring from the dehydration of $Co_3[Co(CN)_6]_2 \cdot 12H_2O$ are presented. This new proposed model which is an outgrowth and improvement of the original model adopted by Milligan et al.[1] also enables one to explain the derived low magnetic moment data for the Co^{2+} in the dehydrated form observed by Shriver and Brown[2] as well as the changes in the visible and vibrational spectra,

(8) G. W. Beall, W. O. Milligan, J. Petrich, and B. I. Swanson, *Inorg. Chem.*, **17**, 2978 (1978).

(9) B. N. Figgis and J. Lewis, *Prog. Inorg. Chem.*, **6**, 1851 (1964).
(10) F. A. Cotton, D. M. L. Goodgame, and M. Goodgame, *J. Am. Chem. Soc.*, **80**, 4600 (1961).
(11) A. Ludi and H. U. Güdel, *Helv. Chim. Acta*, **51**, 2008 (1968).

in a manner that is more consistent with all of the new observed structural data.

Contribution from the National Chemical Research Laboratory, CSIR, Pretoria 0001, South Africa, and the Institute for Physical Chemistry, University of Frankfurt, D 6000 Frankfurt am Main, West Germany

Uncatalyzed Cis to Trans Isomerization of PtX(C$_6$H$_5$)(PEt$_3$)$_2$ Complexes in Methanol. Further Evidence for an Initial Solvolysis Step

WYNAND J. LOUW,[1] RUDI van ELDIK,*[2] and HARTWIG KELM*[2]

Received March 20, 1980

Kinetic data for the uncatalyzed cis to trans isomerization reactions of PtX(C$_6$H$_5$)(PEt$_3$)$_2$ (X = Cl, Br, I) in methanol are reported as a function of the added X$^-$ concentration. The suggested reaction mechanism consists of a rapid preequilibration, during which the solvent-containing intermediate species *cis*-PtS(C$_6$H$_5$)(PEt$_3$)$_2$ is formed, followed by a rate-determining isomerization step. The rate constant for the latter reaction was found to be independent of X with an activation volume of 6.4 ± 0.4, 5.2 ± 0.3, and 7.2 ± 0.8 cm^3 mol^{-1} for X = Cl, Br, and I, respectively, at 30 °C and an ionic strength of 0.01 M. In addition, conductometric data for the preequilibrium step and kinetic data for the substitution reactions of *cis*-PtX(C$_6$H$_5$)(PEt$_3$)$_2$ are reported as further evidence for the suggested mechanism.

Introduction

A dissociative mechanism (Scheme I) has been postulated[3] for isomerization reaction 1, where X = halide and R = alkyl,

$$cis\text{-PtXR(PEt}_3)_2 \xrightarrow{\text{methanol}} trans\text{-PtXR(PEt}_3)_2 \quad (1)$$
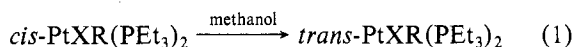
aryl, or substituted aryl. The rate law for the suggested mechanism was derived[3] by applying the steady-state approximation to the *cis*-PtR(PEt$_3$)$_2$ species and is represented by eq 2.

$$k_{obsd} = \frac{k_D k_T}{k_{-D}[\text{X}^-] + k_T} \approx k_D \quad \text{(at low [X}^-]) \quad (2)$$

It was recently proposed[4] that an associative mechanism (Scheme II) should rather be used to explain reaction 1, in which the *cis*-PtXR(PEt$_3$)$_2$ species are present in a fast preequilibrium with the respective *cis*-PtSR(PEt$_3$)$_2$ species. Under such conditions rate law 3 is applicable. In this

$$k_{obsd} = \frac{k_i K_s}{[\text{X}^-] + K_s} \approx k_i \quad \text{(at low [X}^-]) \quad (3)$$
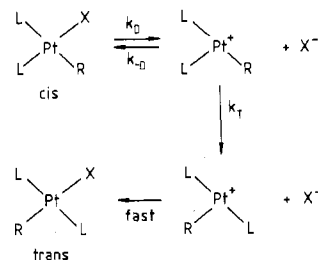
mechanism k_i is the rate-determining step and explains why the isomerization reaction is slower than the solvolysis reaction. It was further proposed[4] that only for the most bulky R group (when the isomerization and solvolysis rates are the same) should a steady state approximation be used, resulting eq 4 such that k_s is now the rate-determining step.

$$k_{obsd} = \frac{k_i k_s}{k_{-s}[\text{X}^-] + k_i} \approx k_s \quad \text{(at low [X}^-]) \quad (4)$$

The following evidence in favor of Scheme II (rate laws 3 and 4) has been reported.

(a) For X = Br and R = Mesityl (Rate Law 4). (i) the isomerization rate constant (in the absence of added Br$^-$, i.e., $k_{obsd} \approx k_s$), $\Delta H^{\ddagger}$, $\Delta S^{\ddagger}$, and $\Delta V^{\ddagger}$ [3–5] agree within experimental error with the relevant parameters found for the solvolysis[3,4]

(1) National Chemical Research Laboratory.
(2) University of Frankfurt.
(3) Romeo, R.; Minnita, D.; Trozzi, M. *Inorg. Chem.* **1976**, *15*, 1134.
(4) van Eldik, R.; Palmer, D. A.; Kelm, H. *Inorg. Chem.* **1979**, *18*, 572.
(5) Kelm, H.; Louw, W. J.; Palmer, D. A. *Inorg. Chem.* **1980**, *19*, 843.

Scheme I

of *cis*-PtBr(mesityl)(PEt$_3$)$_2$. (ii) $\Delta V^{\ddagger}$ values[4,5] of −14 ± 2 cm^3 mol^{-1} and $\Delta S^{\ddagger}$ values[3,4] of −18 ± 4 cal K^{-1} mol^{-1} are consistent with an associative step.

(b) For X = Br and R = Phenyl (Rate Law 3). (i) Semilog plots of optical density change vs. time for reaction 1 deviate from linearity[5] at [complex] > 5 × 10^{-5} M. This is in agreement with a fast preequilibrium step (Scheme II), causing the initial [Br$^-$] to be comparable with the K_s value and, therefore, resulting in a slower initial rate. As the bromide ions are incorporated into the trans product, the [Br$^-$] decreases to a point where [Br$^-$] ≪ K_s such that linearity is obtained in the semilog plots.[5] On the addition of Br$^-$ to the reaction solution, the [Br$^-$] term in rate law 3 becomes constant and no curvature is observed.[5] (ii) From the linear plot of dtc_t/dc vs. $(K_s + 4c_t)^{1/2}$ (dc/dt = initial rate, c_t = initial complex concentration), the k_i value (rate law 3) obtained from the intercept[5] agreed within experimental error limits with those measured independently.[5]

A further crucial experiment in order to distinguish between the mechanisms outlined in Schemes I and II would be to study the influence of different X ligands on the magnitude of the observed isomerization rate constant. k_i (Scheme II, rate law 3) should be independent of the nature of X, whereas large variations are expected for the corresponding k_D or k_s values (Scheme I, rate law 2, or Scheme II, rate law 4). The results of such an investigation are reported in this paper.

Experimental Section

Materials. Methanol was distilled over magnesium. All other chemicals were of analytical reagent grade and dried in vacuo. *cis*-PtX(C$_6$H$_5$)(PEt$_3$)$_2$ (X = Cl, Br) were prepared according to